

# ON THE STRUCTURE AND NATURE OF DARK MATTER HALOS

ANDREAS BURKERT

*Max-Planck-Institut für Astronomie, Königstuhl 17,  
69117 Heidelberg, GERMANY*

JOSEPH SILK

*Department of Astrophysics, NAPL, Keble Rd, Oxford OX1 3RH, UK, and  
Departments of Astronomy and Physics, University of California,  
Berkeley, CA 94720, USA*

The structure of dark matter halos as predicted from cosmological models is discussed and compared with observed rotation curves of dark matter-dominated dwarf galaxies. The theoretical models predict that dark matter halos represent a one-parameter family with a universal density profile. Observations of dark matter-dominated rotation curves indeed confirm the universal structure of dark halos. They are even in excellent agreement with the expected mass-radius scaling relations for the currently favoured cosmological model (standard cold dark matter with  $\Omega_0 = 0.25$  and  $\Omega_\Lambda = 0.75$ ). The rotation profiles however disagree with the predicted dark matter density distributions. Secular processes which might affect the inner halo structure do not seem to provide a good solution to this problem. We discuss, as an alternative, the possibility that dark halos consist of two separate components, a dark baryonic and a dark non-baryonic component.

## 1 Introduction

Cosmological models of hierarchical merging in a cold dark matter universe are in some difficulty. High-resolution N-body simulations (Navarro et al. 1996a; NFW) have shown that the density profiles  $\rho_{NFW}$  of virialized dark matter halos should have a universal shape of the form

$$\rho_{NFW}(r) = \frac{3H_0^2}{8\pi G} \frac{\delta_c}{(r/r_s)(1+r/r_s)^2} \quad (1)$$

where  $r_s$  is a characteristic length scale and  $\delta_c$  a characteristic density enhancement. The two free parameters  $\delta_c$  and  $r_s$  can be determined from the halo concentration  $c$  and the virial mass  $M_{200}$

$$\delta_c = \frac{200}{3} \frac{c^3}{\ln(1+c) - c/(1+c)} \quad (2)$$

$$r_s = \frac{R_{200}}{c} = \frac{1.63 \times 10^{-2}}{c} \left( \frac{M_{200}}{M_\odot} \right)^{1/3} h^{-2/3} kpc. \quad (3)$$

where  $R_{200}$  is the virial radius, that is the radius inside which the average overdensity is 200 times the critical density of the universe and  $M_{200}$  is the mass within  $R_{200}$ .

For any particular cosmology there also exists a good correlation between  $c$  and  $M_{200}$  which results from the fact that dark halo densities reflect the density of the universe at the epoch of their formation (NFW, Salvador-Solé et al. 1998) and that halos of a given mass are preferentially assembled over a narrow range of redshifts. As lower mass halos form earlier, at times when the universe was significantly denser, they are more centrally concentrated. NFW have published concentrations for dark matter halos in the mass range of  $3 \times 10^{11} M_{\odot} \leq M_{200} \leq 3 \times 10^{15} M_{\odot}$  which can be well fitted by the following power-law functions:

$$\begin{aligned} c &= 8.91 \times 10^2 \left( \frac{M_{200}}{M_{\odot}} \right)^{-0.14} & \text{for SCDM} \\ c &= 1.86 \times 10^2 \left( \frac{M_{200}}{M_{\odot}} \right)^{-0.10} & \text{for CDMA} \end{aligned} \quad (4)$$

where SCDM denotes a standard biased cold dark matter model with  $\Omega_0=1$ ,  $h=0.5$ ,  $\sigma_8=0.65$  and CDMA denotes a low-density universe with a flat geometry and a non-zero cosmological constant, defined by  $\Omega_0=0.25$ ,  $\Omega_{\Lambda}=0.75$ ,  $h=0.75$ ,  $\sigma_8=1.3$ . Note that the universal profile (equation 1) and the scaling relations (equation 4) have only been determined from simulations for halo masses as small as  $M_{200} = 10^{11} M_{\odot}$ , but there is no reason to believe that these results would not be valid for halos which are, say, one order of magnitude lower in mass. In summary, dark matter halos represent a one-parameter family, with their density distribution being determined completely by their virial mass  $M_{200}$ .

The universal character of dark matter profiles and the validity of the NFW-profile for different cosmogonies has been verified by many N-body calculations (e.g. Navarro et al. 1997, Cole & Lacey 1997, Tormen et al. 1997, Tissera & Dominguez-Tenreiro 1998, Jing 1999). In one of the highest resolution simulations to date, Moore et al. (1998, see also Fukushige & Makino 1997) found good agreement with the NFW profile (equation 1) at and outside of  $r_s$ . Their simulations did however lead to a steeper innermost slope  $\rho \sim r^{-1.4}$  which extends all the way down to their resolution limit of 0.01  $r_s$ .

On the analytical side, early spherically symmetric collapse models by Gunn & Gott (1972) studied the collapse of a uniformly overdense region. Gott (1975) and Gunn (1977) investigated secondary infall onto already col-

lapsed density perturbations and predicted  $r^{-9/4}$  profiles. Fillmore & Goldreich (1984) found self-similarity solutions for the secondary infall models. Hoffman & Shaham (1985) took into account more realistic Gaussian initial conditions and predicted sharp central density peaks of the form  $\rho \sim r^{-2}$ . An updated version of these models by Krull (1999) abandoned self-similarity and explicitly took into account the hierarchical formation history. His models lead to excellent agreement with the NFW-profile in the radius range  $0.5r_s \leq r \leq 10r_s$ .

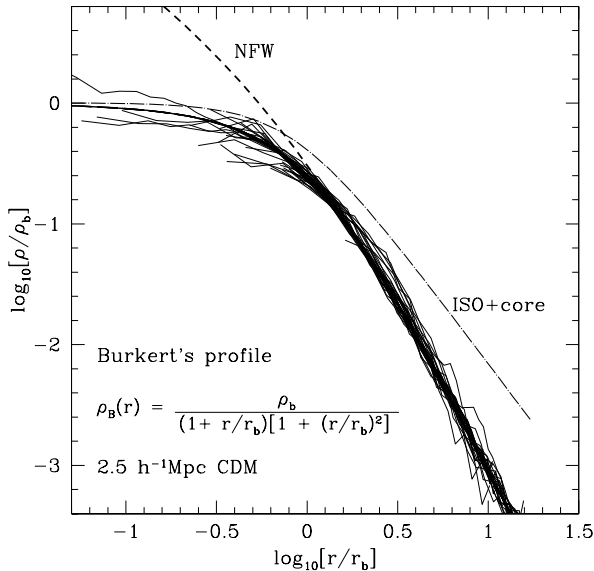


Figure 1: The density distributions of dark halos in a cold dark matter simulation of KKBP (thin solid lines) are compared with the Burkert profile (thick solid line) that provides a good fit to the observed rotation curves of dark matter-dominated dwarf galaxies. The thick dashed line shows the NFW profile which predicts too much dark matter mass inside  $r_b$ . The dot-dashed curve shows an isothermal profile with a finite density core which fails in the outer regions where it decreases as  $r^{-2}$ .

In a different series of very high-resolution models, using a new adaptive refinement tree N-body code, Kravtsov et al. (1998, KKBP) found significant deviations from the NFW profile or an even steeper inner power-law density distribution for  $r \leq 0.5r_s$ . In this region their dark matter profiles show a substantial scatter around an average profile that is characterized by a shallow central cusp with  $\rho \sim r^{-0.3}$ . Although the scatter is large, this result is in

clear contradiction to the simulations of Moore et al. (1998) with equally high central resolution. Figure 1 (adopted from Primack et al. 1998) compares the NFW-profile (dashed line) with the profiles of dark matter halos of KKBP (thin solid lines).

## 2 The dark matter halo of DDO 154

DDO 154 (Carignan & Freeman 1988) is one of the most gas-rich galaxies known with a total H I mass of  $2.5 \times 10^8 M_\odot$  and an inner stellar component of only  $5 \times 10^7 M_\odot$ . Recently, Carignan & Purton (1998) measured the rotation curve of its extended H I disk all the way out to 21 optical disk scale lengths. As the rotation curve, even in the innermost regions, is almost completely dominated by dark matter, this galaxy provides an ideal laboratory for testing the universal density profile predictions of cosmological models.

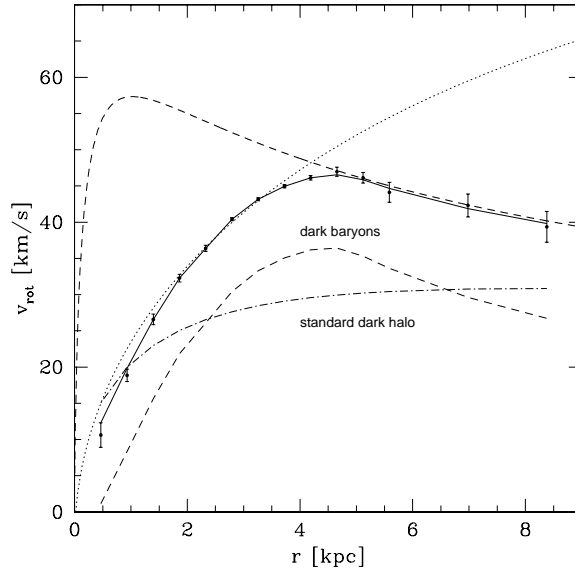


Figure 2: The dark matter rotation curve of DDO 154 with error bars. The dotted line is a fit to the inner parts, adopting a NFW profile. The dashed curve shows a fit to the outer regions. The solid line shows the fit which is achieved with a two-component model where the lower dashed line shows the contribution of the dark baryonic component and the lower dot-dashed curve is the standard dark matter halo contribution adopting a NFW profile.

Figure 2 shows the dark matter rotation curve of DDO 154 and compares

it with the NFW profile. Note that the maximum rotational velocity  $v_{max} \approx 47$  km/s is reached at a radius of  $r_{max} \approx 4.5$  kpc, beyond which the rotation decreases again. Fitting the inner regions (dotted line) has been known to pose a problem (Flores & Primack 1994, Moore 1994, Burkert 1995). However an even larger problem exists in the outermost regions where far too much dark matter would be expected. The dashed line in figure 2 shows a fit to the outer regions. In this case, the dark matter excess in the inner regions is unacceptably large. We conclude that the well-studied dark matter rotation curve of DDO 154 is far from agreement with NFW profiles.

We can also compare the observed location  $r_{max}$  and the value  $v_{max}$  of the observed maximum rotational velocity with predictions of a SCDM model. Adopting a NFW profile, the virial radius is determined by  $R_{200} = 0.5 c r_{max}$ . The virial mass is then given by the relation

$$1.63 \times 10^{-2} \left( \frac{M_{200}}{M_{\odot}} \right)^{1/3} h^{-2/3} = \left( \frac{R_{200}}{\text{kpc}} \right) = 0.5c \left( \frac{r_{max}}{\text{kpc}} \right). \quad (5)$$

Adopting the SCDM model with  $h=0.5$  and inserting equation (4) for  $c$  one obtains

$$M_{200}^{SCDM} = 9 \times 10^8 \left( \frac{r_{max}}{\text{kpc}} \right)^{2.11} M_{\odot} \quad (6)$$

For DDO 154 with  $r_{max} = 4.5$  kpc we find  $M_{200} = 2.1 \times 10^{10} M_{\odot}$ ,  $R_{200} = 72$  kpc and  $c = 31.9$ . For these halo values, the predicted maximum rotational velocity would be

$$v_{max} = 0.465 \left( \frac{c}{\ln(1+c) - c/(1+c)} \right)^{1/2} h \left( \frac{R_{200}}{\text{kpc}} \right) = 60 \text{ km/s} \quad (7)$$

which is a factor 1.3 larger than observed.

Adopting instead the CDMA model with  $h=0.75$ , a similar calculation leads to

$$M_{200}^{CDMA} = 3 \times 10^8 \left( \frac{r_{max}}{\text{kpc}} \right)^{2.3} M_{\odot} \quad (8)$$

and therefore to  $M_{200} = 9.5 \times 10^9 M_{\odot}$ ,  $R_{200}=42$  kpc,  $c=18.7$  and  $v_{max}=44.4$  km/s which is in excellent agreement with the observations (47 km/s), especially if one notes that equation 4 has been verified only for viral masses of  $M_{200} > 10^{11} M_{\odot}$ .

In summary, the radius and mass scale of DDO 154 as determined from the value and location of its maximum rotational velocity is in perfect agreement with the predictions of the currently most favoured cosmological models (CDM $\Lambda$ ). The inferred dark matter density distribution is however quite different.

### 3 The universality of observed dark matter mass profiles.

DDO 154 is not a peculiar case. Burkert (1995) showed that the dark matter rotation curves of four dwarf galaxies studied by Moore (1994) have the same shape which can be well described by the density distribution

$$\rho_B(r) = \frac{\rho_b}{(1 + r/r_b)[1 + (r/r_b)^2]}. \quad (9)$$

KKBP extended this sample to ten dark matter-dominated dwarf irregular galaxies and seven dark matter-dominated low surface brightness galaxies. As shown in figure 3 *all* have the same shape, corresponding to a density distribution given by equation (9) and in contradiction to equation (1).

Equation 9 predicts a flat dark matter core, the origin of which is difficult to understand in the context of hierarchical merging (Syer & White 1998) as lower-mass dark halos in general have high densities and therefore spiral into the center of the more diffuse merger remnant, generating high-density cusps.

There is a fundamental difference in the kinematical properties of dark matter halos described by NFW profiles and Burkert profiles (equation 9). Assuming isotropy and spherical symmetry in the inner regions, the Jeans equation predicts a velocity dispersion profile  $\sigma(r)$  of NFW halos that decreases towards the center as  $\sigma \sim r^{1/2}$  (see also the simulations of Fukushige & Makino 1997) whereas Burkert halos have isothermal cores with constant velocity dispersion. Again, non-isothermal, kinematically cold dark matter cores might be expected in hierarchical merging scenarios as the denser clumps that sink towards the center of merger remnants have on average smaller virial dispersions.

### 4 On the origin of dark matter cores

It is rather unsatisfying that numerical studies of dark matter halos using different techniques lead to different results. KKP find dark matter halo profiles that, on average, can be well fitted by a Burkert profile (Fig. 1) and therefore also provide a good fit to observed rotation curves. The NFW-profiles, or even steeper inner density gradients (Moore et al. 1998) seem to be in clear conflict with observations (Fig. 2). Numerical resolution cannot be the answer

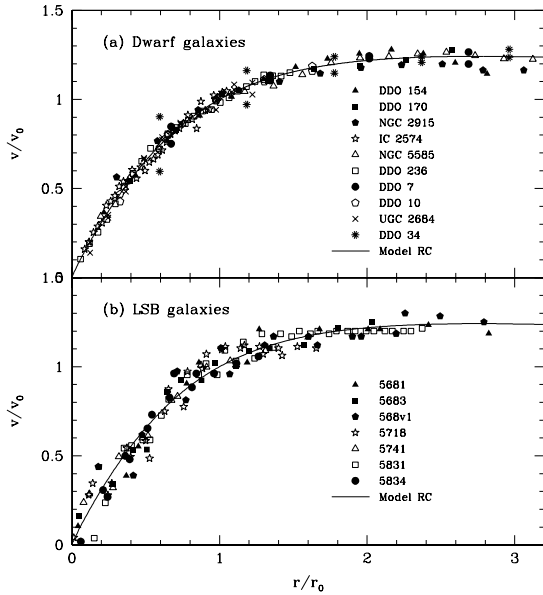


Figure 3: This figure, adopted from Primack et al. (1998) shows the dark matter rotation curves of (a) ten dwarf irregular and (b) seven low surface brightness galaxies. The solid line shows the profile proposed by KKPB which is nearly identical to  $\rho_B$  (equation 9).

as the N-body simulations of Moore et al. (1998) have enough resolution to determine the dark matter density distribution within  $0.5 r_s$ , where any flattening should have been found. Instead, the authors find profiles that are even steeper than  $r^{-1}$ . One should note that the results of KKPB have not yet been reproduced by other groups, whereas dark profiles with central  $r^{-1}$  profiles or even steeper cusps have been found independently in many studies using different numerical techniques. On the other hand, the high-resolution studies of KKPB sample galactic halos, whereas most of the other studies simulate halos of galactic clusters. Indeed, there exists observational evidence that the dark matter distribution in clusters of galaxies is well described by NFW profiles (Carlberg et al. 1997, McLaughlin 1999). One conclusion therefore could be that dark matter halos are not self-similar but that their core structure does depend on their virial mass. Because one is sampling different parts of the primordial CDM density fluctuation power spectrum, from which the initial

conditions are derived, it is possible that the initial conditions could influence the final result. For example, low mass dark halos have initial fluctuations which result in virialized velocity dispersions that are nearly independent of mean density, and so a hierarchy of substructure would be expected to be nearly isothermal. For more massive halos typical of normal galaxies, the velocity dispersion varies as  $\rho^{\frac{n-1}{3(n+3)}}$  where  $n$  is the effective power-law power spectrum index  $\delta\rho/\rho \propto M^{-\frac{n+3}{6}}$  and  $n \approx -2$  on galaxy scales but  $n \approx -3$  for dwarfs. Low-mass dark halos could then indeed have isothermal, constant density cores whereas high-mass dark halos should contain non-isothermal, cold power-law cores. However, even in this case, one still has the problem that the simulations lead to a much greater dispersion of the inner radial profiles than expected from observed rotation curves. Additional effects might therefore be important that have not been taken into account in dissipationless cosmological simulations.

#### 4.1 Secular dynamical processes

Cold dark matter cores with steep density cusps are very fragile and can easily be affected by mass infall and outflow. This has been shown, for example, by Tissera & Domínguez-Tenreiro (1998) who included gas infall in their cosmological models and found even steeper power-laws in the central regions than predicted by purely dissipationless merging due to the adiabatic contraction of the dark component. In order to generate flat cores through secular processes, Navarro et al. (1996b) proposed a scenario where after a slow growth of a dense gaseous disk the gas is suddenly ejected. The subsequent expansion and violent relaxation phase of the inner dark matter regions leads to a flattening of the core. This model has been improved by Gelato & Sommer-Larsen (1999) who applied it to DDO 154 and found that it is not easy to satisfactorily explain the observed rotation curve even for extreme mass loss rates. In fact, it is unlikely that DDO 154 lost any gas, given its large gas fraction. In addition, secular dynamical processes due to mass outflow would predict inner dark matter profiles that depend sensitively on the detailed physics of mass ejection and therefore should again show a wide range of density distributions, and these are not observed.

#### 4.2 A second dark and probably baryonic component

The rotation curves of the galaxies shown in figure 3 clearly cannot be understood by including only the visible component. It may well be that some non-negligible and as yet undetected fraction of the total baryonic mass con-

tributes to their dark component, in addition to the non-baryonic standard cold dark component that is considered in cosmological models.

In fact, there is ample room for such a dark baryonic component. Primordial nucleosynthesis requires a baryonic density of  $\Omega_b h^2 \approx 0.015 \pm 0.008$  (Kurki-Suonio et al. 1997, Copi et al. 1995), whereas the observed baryonic density for stellar and gaseous disks lies in the range of  $\Omega_d \approx 0.004 \pm 0.002$  (Persic & Salucci 1992). Moreover modelling of Lyman alpha clouds at  $z \sim 2 - 4$  suggests that all of the baryons expected from primordial nucleosynthesis were present in diffuse form, to within the uncertainties, which may amount to perhaps a factor of 2 (Weinberg et al. 1997). Hence dark baryons are required at low redshift. These may be in the form of hot gas that must be mostly outside of systems such as the Local Group and rich galaxy clusters (Cen and Ostriker 1999). But an equally plausible possibility is that the dark baryons are responsible for a significant fraction of the mass in galaxy halos, as is motivated by arguments involving disk rotation curves and halo morphologies (cf Gerhard and Silk 1996; Pfenniger et al. 1994).

This second dark baryonic component could be diffuse  $H_2$  within the disks or some spheroidal distribution of massive compact baryonic objects (MACHOs), comparable to those that have been detected via gravitational microlensing events towards the Large Magellanic Cloud (LMC). It is difficult to reconcile the inferred typical MACHO lens mass of  $\sim 0.5 \pm 0.3 M_\odot$ , as derived from the first 2.3 years of data for 8.5 million stars in the LMC (Alcock et al. 1996), with ordinary hydrogen-burning stars or old white dwarfs (Bahcall et al. 1994, Hu et al. 1994, Carr 1994, Charlot & Silk 1996). Brown dwarfs, substellar objects below the hydrogen-burning limit of  $0.08 M_\odot$  would be ideal candidates. Indeed, halo models can be constructed, e.g. by assuming a declining outer rotation curve, for which the most likely MACHO mass is  $0.1 M_\odot$  or less (Honma & Kan-ya 1999) with a MACHO contribution to the total dark mass of almost 100%. Freese et al. (1999) have however shown by deep star counts using HST that faint stars and massive brown dwarfs contribute no more than 1% of the expected total dark matter mass density of the Galaxy, ruling out such a low-mass population.

A simple explanation of the MACHO mass problem has been presented by Zaritsky & Lin (1997) and Zhao (1998), who argued that the MACHOs reside in a previously undetected tidal stream, located somewhere in front of the LMC. In this case the microlensing events would represent stellar objects in the outer regions of the LMC and would not be associated with a dominant dark matter component of the Milky Way. This solution is supported by the fact that all lensing events toward the LMC and SMC with known distances (e.g. the binary lensing event 98 LMC-9, or 98-SMC-1) appear to be a result of

self-lensing within the Magellanic Clouds. However the statistics are abysmal: only two SMC events have been reported, and there are approximately 20 LMC events in all, of which two have known distances. Moreover one can only measure distances for binary events, and these are very likely due to star-star lensing. Finally, the SMC is known to be extended along the line of sight, thereby enhancing the probability of self-lensing.

Thus, while evidence for a possible dark baryonic component in the outer regions of galaxies is small, such a component could still be the solution to the dark matter core problem. Burkert & Silk (1997) showed that the observed rotation curve of DDO 154 could be reconciled with standard cosmological theories if, in addition to a standard dark matter halo with an NFW-profile (corrected for adiabatic contraction), a separate and centrally condensed dark baryonic component is introduced. The solid line in figure 2 shows the fit achieved with the 2-component dark model of Burkert and Silk adopting dark matter halo parameters which are in agreement with CDMA models and using a spherically symmetric dark baryonic component with a physically reasonable density distribution that decreases monotonically with increasing radius. The required mass of the dark baryonic spheroid is  $1.5 \times 10^9 M_\odot$  which is 4-5 times the mass of the visible gaseous galactic disk and about 25% the total mass of the non-baryonic dark component. The apparent universality of rotation curves would then suggest that the relative mix of the two dark components should in turn be universal. The origin of such a dark baryonic component which must have formed during an early dissipative condensation phase of baryons relative to the nondissipative, collisionless dark matter component is not understood. However this is not to say that it could not have occurred. Our understanding of early star formation and the primordial initial mass function is sufficiently primitive that this remains very much an open possibility.

## References

1. C. Alcock et al., *Astrophys. J.*, **461**, 84 (1996).
2. J.N. Bahcall, C. Flynn, A. Gould, S. Kirhakos, *Astrophys. J.*, **435**, L51 (1994).
3. A. Burkert, *Astrophys. J.*, **447**, L25 (1995).
4. A. Burkert and J. Silk, *Astrophys. J.*, **488**, L55 (1997).
5. C. Carignan and K.C. Freeman, *Astrophys. J.*, **332**, L33 (1988).
6. C. Carignan and C. Purton, *Astrophys. J.*, **506**, 125 (1998).
7. R.G. Carlberg et al., *Astrophys. J.*, **485**, L13 (1997).
8. B. Carr, *ARA&A*, **32**, 531 (1994).
9. R. Cen and J. P. Ostriker, *Astrophys. J.*, in press

10. S. Charlot and J. Silk, *Astrophys. J.*, **445**, 124 (1996).
11. S. Cole and C. Lacey, *MNRAS*, **281**, 716 (1997).
12. C.J. Copi, D.N. Schramm, M.S. Turner, *Science*, **267**, 192 (1995).
13. K. Freese, B. Fields, D. Graff, *astro/ph9901178* (1999).
14. T. Fukushige and J. Makino, *Astrophys. J.*, **477**, L9 (1997).
15. J.A. Fillmore and P. Goldreich, *Astrophys. J.*, **281**, 1 (1984).
16. R.A. Flores and J.R. Primack, *Astrophys. J.*, **427**, L1 (1994).
17. S. Gelato and J. Sommer-Larsen, *MNRAS*, **303**, 321 (1999).
18. O. Gerhard and J. Silk, *Astrophys. J.*, **472**, 34 (1996)
19. J.R. Gott, *Astrophys. J.*, **201**, 296 (1975)
20. J. Gunn and J.R. Gott, *Astrophys. J.*, **209**, 1 (1972).
21. J. Gunn, *Astrophys. J.*, **218**, 592 (1977).
22. Y. Hoffman and J. Shaham, *Astrophys. J.*, **297**, 16 (1985).
23. M. Honma and Y. Kan-ya, *Astrophys. J.*, **503**, L139 (1998).
24. E.M. Hu, G. Gilmore, L.L. Cowie, *Nature*, **371**, 493 (1994).
25. Y.P. Jing, *astro-ph/9901340* (1999)
26. A.V. Kravtsov, A.A. Klypin, J.S. Bullock and J.R. Primack, *Astrophys. J.*, **502**, 48 (1998), KKBP
27. A. Krull, *astro-ph/9902299* (1999)
28. H. Kurki-Suonio, K. Jedamzik, G.J. Mathews, *Astrophys. J.*, **479**, 31 (1997)
29. D.E. McLaughlin, *Astrophys. J.*, **512**, L9 (1999)
30. B. Moore, *Nature*, **370**, 629 (1994).
31. B. Moore, F. Governato, T. Quinn, J. Stadel and G. Lake, *Astrophys. J.*, **499**, L5 (1998)
32. J.F. Navarro, C.S. Frenk and S.D.M. White, *Astrophys. J.*, **462**, 563 (1996a), NFW
33. J.F. Navarro, V.R. Eke, C.S. Frenk, *MNRAS*, **283**, L72 (1996b).
34. J.F. Navarro, C.S. Frenk and S.D.M. White, *Astrophys. J.*, **490**, 493 (1997)
35. M. Persic and O. Salucci, *MNRAS*, **258**, 14 (1992)
36. D. Pfenniger, F. Combes and L. Martinet, *Astron. & Astrophys. J.*, **285**, 79 (1994)
37. J.R. Primack, J.S. Bullock, A.A. Klypin, A.V. Kravtsov, *astro-ph/9812241*, (1998)
38. E. Salvador-Solé, J.M. Solanes and A. Manrique, *Astrophys. J.*, **499**, 542 (1998)
39. D. Syer and S.D.M. White, *MNRAS*, **293**, 337 (1998)
40. P.B. Tissera and R. Domínguez-Tenreiro, *MNRAS*, **297**, 177 (1998)
41. G. Tormen, F.R. Bouchet and S.D.M. White, *MNRAS*, **286**, 865 (1997)

42. D. Weinberg, J. Miralda-Escude, L. Hernquist and N. Katz, *Astrophys. J.*, **490**, 564 (1997)
43. D. Zaritsky and D.N.C. Lin, *Astron. J.*, **114**, 2545 (1997)
44. H.S. Zhao, *MNRAS*, **294**, 139 (1998)